INTERACTIVE CONTROL ENGINEERING
Principles and Applications

Volume 5 Delays, Slow Measurements, and State Estimation

CHAPTER 11

Controlling an Unmeasured Product Temperature in a Multi-Zone Cathode Calcination Kiln

Pages 269–293

Edited by John D. Hedengren

How to cite this chapter. "Controlling an Unmeasured Product Temperature in a Multi-Zone Cathode Calcination Kiln," in *Delays, Slow Measurements, and State Estimation*, John D. Hedengren, Ed., vol. 5 of *Interactive Control Engineering: Principles and Applications*. Advanced Process Solutions, LLC, 2026, ch. 11, pp. 269–293.

The page numbers in this file are those of the printed volume.

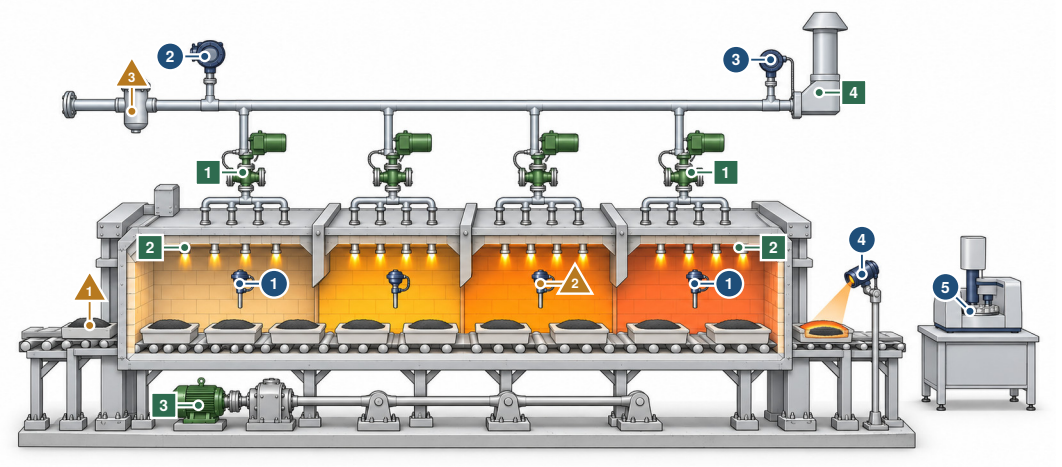
The app for this chapter
https://apmonitor.com/apps/cathode-kiln/

The volume online: contents, other chapters and citation records
https://apmonitor.com/apps/books/v05-delays-estimation/#cathode-kiln

Copyright © 2026 Advanced Process Solutions, LLC. All rights reserved. Produced by Advanced Process Solutions, LLC.

CHAPTER 11

Controlling an Unmeasured Product Temperature in a Multi-Zone Cathode Calcination Kiln



The controller moves 1 gas valves: oxygen share of the blend 2 zone heaters 3 conveyor drive: line speed 4 exhaust damper

The controller reads 1 zone thermocouples, one per zone 2 oxygen in the firing section 3 kiln pressure 4 exit pyrometer on the brick surface 5 laboratory assay, six hours late

What disturbs it 1 denser or wetter bricks 2 a thermocouple that reads high 3 oxygen supply cut back

No instrument reaches the middle of a brick, so the controllers hold the zone readings (1) while the core is estimated from a model and checked only at the exit (4) and in the laboratory (5). Illustration, not to scale.

IN PLAIN TERMS A Kiln Whose Most Important Temperature Is Hidden

The main idea. A long electric oven bakes pressed bricks of powder for more than a day. The baked powder becomes part of a battery. Each section of the oven has its own thermometer and heater. The middle of each brick, where the chemistry happens, has no thermometer at all.

The challenge. The oven can sit right on its settings while the brick centers lag behind, like a thick roast still cold inside a hot oven. The plant must guess the center from a model. A faster belt also leaves less time for the slowest change to finish.

Why it matters. Past a certain belt speed, every brick fails its test.

THREE WAYS TO READ THIS CHAPTER

Explore	11 min	the first page, the history and the fact on the cathode (Section 11.1), the try-it on the biased thermocouple and the try-it on the two cascades, the fact on line speed (Section 11.5) and the key points
Study	45 min	the whole chapter with its three pause points and the twelve exercises at its end
Practice	15 min	the first page, the results (Section 11.5), Technology in Practice (Section 11.6), Limitations (Section 11.7) and the open challenge

The control question A cathode kiln fires compacted bricks for thirty hours, and the core temperature that sets their reactions has no instrument on it. How much of that core do ten well-tuned zone loops control, what does an estimator of the core add, and how fast can the line run before the material leaves the kiln off specification?

Learning objectives

- Compute the parcel mass, residence time and transport delays of the kiln from the conveyor speed, and the surface and core time constants of the brick.
- Identify a zone from a manual step test, and contrast its gain and lag with those of the brick core.
- Explain how a zone loop on setpoint, a biased thermocouple or a surface cascade can leave the product off specification, and name the measurement that reveals each.
- Compare a surface cascade with a core cascade on a soft-sensed temperature, and state which direction of estimator error is dangerous.
- Locate the line speed at which good production peaks, and name the constraint that binds there.

Prerequisites Sections 1.4.4 (delay that moves with flow, material tracking), 1.4.2 (fitted dead time), 1.4.6 (observability), 1.4.8 (soft sensors) and 1.6.2 (velocity-form PID), and Chapter 10 for a quality controlled through an inferred variable.

The app https://apmonitor.com/apps/cathode-kiln/

See also Volume 3, Chapter 2 for choosing the inner measurement of a cascade, Volume 3, Chapter 3 for the speed an inner loop must reach, and Volume 3, Chapter 6 for feedforward from an upstream measurement when feedback sits hours behind the dose.

11.1 Introduction

The thermal processing step that turns a blended precursor into a layered oxide cathode is the most capital-intensive operation in a battery material plant and the one that sets what the plant can make [1]. A nickel-manganese-cobalt hydroxide precursor is blended dry with lithium hydroxide monohydrate, compacted, and fired through a staged thermal cycle under a controlled atmosphere before being cooled, crushed and classified [2, 3]. The properties that a cell eventually reports, the degree of lithiation, the extent of layered ordering, the amount of lithium and nickel site mixing and the quantity of residual lithium left on the particle surface, are all set by the temperature and atmosphere history the material receives inside that kiln [4, 5].

> ⧖ HISTORY **1980: A Layered Oxide Becomes a Cathode**
>
> In 1979 and 1980 John B. Goodenough and his co-workers at Oxford University found that a lithium cobalt oxide could serve as the cathode, the positive electrode, of a lithium battery. Its cobalt dioxide layers are separated by gaps in which lithium ions can be bound without a dramatic expansion of the lattice, and the material showed a very high potential of about 4 to 5 volts against lithium. Paired with a carbon anode, it was the cathode of the commercial lithium battery released in 1991, and new cathode materials have been found since for particular uses [6]. The nickel-rich material this chapter's kiln fires is a layered oxide of the same kind [2].

That history is not measured. A kiln carries a thermocouple in each zone, and a thermocouple reads the zone. Compaction, which is the cheapest capacity a cathode plant can buy because it puts roughly three times as much material in the same machine, is what separates the two: a dense brick has an interior, and that interior is minutes of surface lag and tens of minutes of conduction behind the wall that is heating it. Full-scale modeling of an industrial roller hearth kiln firing ternary precursors reports exactly this separation between the gas and wall temperatures a kiln instrument sees and the temperatures the material containers experience, together with the dependence of that separation on loading and residence time [7].

The class of problem is not confined to batteries. Any continuous furnace that carries a thick charge through a graded profile has an unmeasured product temperature behind a transport delay, and the established answer is a model-based estimate of the material rather than a better measurement of the furnace. Strip temperature in a continuous annealing line was controlled that way from the middle 1990s [8], and the current generation of those controllers is a nonlinear model predictive layer over a distributed thermal model of the strip and the furnace [9, 10]. Kiln control has a parallel history: model predictive control was commissioned on industrial lime kilns in the 1990s against the same combination of long transport delay and slow laboratory feedback [11], and computational fluid dynamics is now routine for the calcination reaction inside them [12]. In both industries the useful measurement of the product is inferred rather than sensed, which places the problem squarely in the soft-sensor literature [13].

Simulation is where the separation can be seen, because on a real kiln the core temperature is exactly as invisible to the engineer as it is to the operator. Assessments of process control education call for practice on the plants that industrial practice actually presents [14, 15], and a cathode kiln is such a plant: a perfectly tuned regulatory layer demonstrably fails to control the variable that matters.

The kiln needs more than a better estimator. It is also the bottleneck of the plant, which makes the conveyor speed the manipulated variable with economic consequence, and every percent of line speed shortens the residence time that the slowest reaction needs. Maximum throughput and maximum saleable throughput are therefore different operating points, and the distance between them is set by a reaction rate inside a brick.

> ✦ DID YOU KNOW? **The Heaviest and Costliest Part of the Cell**
>
> The cathode is normally the largest component of a lithium-ion cell by both weight and cost. For commercial nickel-manganese-cobalt cathodes, raw materials make up 75 to 90 percent of the total cost, and further savings can come from the yield and throughput rate of production [2].

This chapter works with a reduced-order kiln model that connects the measurements and manipulated variables of a multi-zone calcination kiln to the inaccessible thermal and reaction history inside a compacted cathode brick, and uses it to quantify the throughput and quality trade-off of a bottleneck unit. Section 11.2 sets out the chemistry of the firing and the shape of the control problem. Section 11.3 develops the model: Lagrangian material parcels, their coupling to the zones, the two-node brick, five reactions, four quality accumulators and the zone, atmosphere and pressure balances. Section 11.4 builds five control layers, from ten zone loops identified by a step test through a throughput feedforward and a cascade on a soft-sensed brick temperature to a supervisory optimizer that sets the line speed. Section 11.5 measures the separation between kiln and product, nine case studies, a sweep of the conveyor speed and the graded challenge. Section 11.6 sets the plant's instruments, heaters and control platform beside the model. Sections 11.7, 11.8 and 11.9 state the limitations, discuss what the results generalize to and summarize them, and Section 11.10 holds the exercises.

11.2 Background

A representative route to nickel-rich cathode active material has five steps. The hydroxide precursor and lithium hydroxide monohydrate are blended dry at a lithium to transition-metal ratio slightly above one, typically 1.03 to 1.05, because lithium is lost during firing. The blend is compacted. The compacts are fired through a long multi-stage thermal cycle. The product is cooled, crushed and classified, and is sometimes washed or surface treated afterward. Published firing cycles for this chemistry span roughly one to one and a half days, so the thirty-hour cycle used here is a design basis for the application rather than a universal recipe.

The chemistry of the firing is not one reaction. Thermal analysis of a nickel-rich hydroxide precursor blended with lithium hydroxide monohydrate resolves distinct events rather than a single

transformation, beginning with the loss of hydrate water near 100 °C, continuing through decomposition of the transition-metal hydroxide near 250 °C and transformation of the lithium hydroxide above 400 °C, and ending with oxidation and lithiation that extend over a much wider temperature range [3]. The layered ordering that follows is slow, strongly activated, and dependent on the oxygen available to it, which is why nickel-rich material is fired under oxygen rather than air and why the oxygen stoichiometry and the defect population respond to the synthesis atmosphere [5].

Two failure modes bracket the firing window from either side. Too little temperature or too little time leaves the layered ordering incomplete and the lithium and nickel sites mixed. Too much of either costs lithium, grows the primary particles and degrades the material in a different way, so the usable window is narrow [2, 4]. A third failure has nothing to do with the firing at all. Residual lithium left on the surface of a nickel-rich particle reacts with atmospheric carbon dioxide and moisture to form lithium carbonate and lithium hydroxide, and it does so preferentially while the product is cooling [16, 17]. The atmosphere control of the cooling section is therefore a quality loop rather than a housekeeping one, and the instrument that finds a fault in it is a dew-point or carbon dioxide analyzer, not a thermocouple.

Against that chemistry, the control problem has the shape of a continuous annealing furnace rather than a stirred tank. The manipulated variables are fast, the measured variables are intermediate, the controlled variable is slow and unmeasured, and the evidence is a laboratory assay taken hours after the material has left. The class was recognized early in steel processing, where model-based strip temperature control replaced furnace temperature control because holding the furnace did not hold the strip [8], and where the current controllers coordinate a distributed thermal model with the line speed in one optimization [10].

11.3 Process Model

The modeled kiln is 40 m long and is divided into ten electrically heated zones of 4 m, each with its own thermocouple, heater and controller, as shown in Figure 11.1. Green compacts travel through it on rollers in eight parallel lanes. The gas space is divided by curtains into three sections that each vent separately, with the gas moving counter-current to the material inside each section.

11.3.1 Variables

Table 11.1 classifies the variables. The ten zone temperatures, the firing-section oxygen fraction and the kiln pressure are measured and controlled. The product temperatures, the reaction extents and the quality index are controlled in the sense that the plant exists to produce them, and none of the three is available to a controller in real time.

🕮 **Pause.** Try Exercise 11.1 before reading on.

11.3.2 Material Transport

Material is carried as $N_C = 40$ Lagrangian parcels, each holding the bricks that occupy one meter of conveyor across all eight lanes, the tracking of material that Section 1.4.4 describes. The parcels share one phase variable rather than forty positions, so their spacing cannot drift, as shown in Equation (11.1).

$$\frac{\mathrm{d}\varphi}{\mathrm{d}t} = v, \qquad x_k = \varphi + k\,p_c + \tfrac{1}{2}p_c, \qquad p_c = \frac{L_K}{N_C} \tag{11.1}$$

where x_k is the center of parcel k and $p_c = 1\,\mathrm{m}$ is the parcel pitch. When φ reaches one pitch the leading parcel has left the kiln, its quality is scored into the campaign ledger, the array is shifted by one index, and a new parcel enters. The new parcel is not given the feed state, because its center is already half a pitch inside the kiln. It is given the feed marched over that half pitch, which makes the traveling wave periodic rather than approximately so.

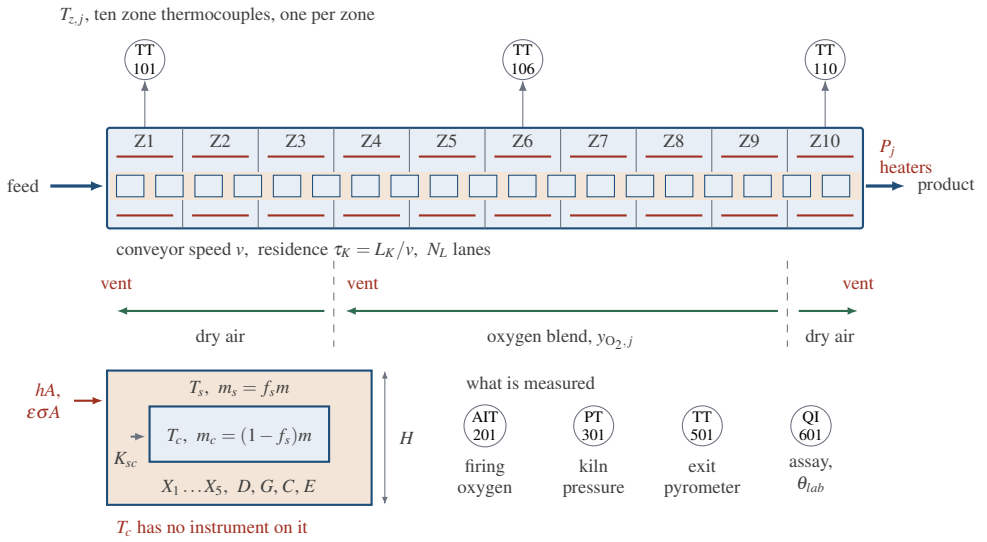


Figure 11.1 Ten-zone cathode calcination kiln, the two-node brick, and the instruments. Each zone carries a thermocouple and a heater, and three gas sections vent separately with the gas counter-current to the material. Ten zone temperatures, one oxygen analyzer, one pressure transmitter, one exit pyrometer and a laboratory assay six hours behind the kiln are the whole instrument list, and the core temperature that sets the reaction rates is not on it.

The mass of a parcel is independent of the line speed, as shown in Equation (11.2), because a faster belt carries the same bricks past faster.

$$m = \frac{N_L \rho_b V_b p_c}{p_b}, \qquad \dot{m} = \frac{m v}{p_c}, \qquad \tau_K = \frac{L_K}{v} \tag{11.2}$$

where $N_L = 8$ lanes, $p_b = 0.34\,\text{m}$ is the brick pitch along the belt and $V_b = 0.0045\,\text{m}^3$ is the brick volume. At $\rho_b = 2500\,\text{kg/m}^3$ each brick is 11.25 kg, each parcel is 264.7 kg, and the design speed gives $\tau_K = 30.0\,\text{h}$ with 353 kg/h of green compact entering. The consequence of the first identity in (11.2) is that raising the line speed is not a larger instantaneous heat load. It is a larger required heating rate, and the zone duty rises only because the material falls further behind the profile.

11.3.3 Coupling Between Parcels and Zones

A ten-zone kiln is not ten isothermal boxes. The muffle, the setters and the gas conduct along the machine, so the environment a brick sees varies smoothly with position while the thermocouple reads it at the middle of its own zone. Each parcel is therefore coupled to the two nearest zone centers in inverse proportion to its distance from them, as shown in Equation (11.3).

$$u = \frac{x_k}{L_z} - \frac{1}{2}, \quad j = \lfloor u \rfloor, \quad w_j = 1 - (u - j), \quad w_{j+1} = u - j \tag{11.3}$$

where $L_z = 4\,\text{m}$ is the zone length. The weighting is a triangular kernel of half-width one zone, sampled on a lattice of one-meter parcels, so it sums to exactly four parcels per zone at every value of φ. Without that property every zone takes a step in loading each time a brick crosses a boundary, and ten zones full of bricks produce a permanent sawtooth on every temperature trend.

Convection sees the linear mean of the two zone temperatures and radiation does not, because the fourth power of an average is not the average of fourth powers. The radiative environment is therefore

Table 11.1 Variable classification

Symbol	Meaning	Units	Range
Controlled, measured			
$T_{z,j}$	zone temperature, $j = 1 \dots 10$	°C	25–880
y_{O_2}	oxygen in the firing section	%	21–98
P	kiln gauge pressure	Pa	−20–80
Controlled, not measured			
T_s	brick surface temperature	°C	25–800
T_c	brick core temperature	°C	25–800
X_4	lithiation extent at the exit	–	0–1
X_5	layered ordering at the exit	–	0–1
Q	CAM quality index	–	0–100
Manipulated			
u_j	zone heater command	%	0–100
f	oxygen share of the gas blend	%	0–100
u_{ex}	exhaust damper	%	5–100
v	conveyor speed	% of design	60–170
$T_{z,j}^{\mathrm{SP}}$	zone setpoint profile	°C	recipe ±
Disturbances			
ρ_b	brick density	×	0.85–1.20
w	free moisture on the feed	×	0.7–1.8
T_{dew}	process-air dew point	°C	−60–20
y_{CO_2}	process-air carbon dioxide	ppm	5–1500
η_6	zone 6 heater rating	×	0.4–1
ϕ_{O_2}	oxygen supply capacity	×	0.4–1
F_{leak}	seal in-leakage	mol/min	0–120
b	thermocouple bias	°C	−25–25

the fourth-power mean of Equation (11.4).

$$T_r = \left[w_j (T_{z,j} + T_0)^4 + w_{j+1} (T_{z,j+1} + T_0)^4 \right]^{1/4} - T_0 \tag{11.4}$$

with $T_0 = 273.15\,\mathrm{K}$. In the annealing ramp, where adjacent zone setpoints differ by 250 °C, using the linear mean in place of (11.4) reports a brick surface tens of degrees too cold and inflates the accumulated gradient penalty more than threefold.

11.3.4 Two-Node Brick

Every parcel carries a surface node holding a fraction $f_s = 0.35$ of the mass and a core node holding the rest, joined by one effective conductance, as shown in Equations (11.5) and (11.6).

$$\begin{aligned} m_s C_p \frac{\mathrm{d}T_s}{\mathrm{d}t} &= hA\,(T_z - T_s) + \varepsilon\sigma A \left[(T_r + T_0)^4 - (T_s + T_0)^4 \right] \\ &\quad - K_{sc}(T_s - T_c) - m_s \textstyle\sum_i \Delta H_i \dot{X}_i \end{aligned} \tag{11.5}$$

$$m_c C_p \frac{\mathrm{d}T_c}{\mathrm{d}t} = K_{sc}(T_s - T_c) - m_c \textstyle\sum_i \Delta H_i \dot{X}_i \tag{11.6}$$

where $m_s = f_s m$ and $m_c = (1 - f_s) m$ are the two node masses, A is the exposed area of the parcel, h the gas convection coefficient, ε the emissivity and σ the Stefan-Boltzmann constant. The conductance

is the lumped Fourier expression of Equation (11.7).

$$K_{sc} = \frac{k_{eff} A_{eff}}{L_{eff}}, \qquad A_{eff} = 2 n_b L W, \qquad L_{eff} = \frac{H}{4} \tag{11.7}$$

where $n_b = 23.5$ is the number of bricks in a parcel, L, W and H are the brick dimensions, and L_{eff} is the distance from a face to the centroid of the half it feeds. With the default geometry $A = 3.18\,\mathrm{m}^2$, $K_{sc} = 6.86\,\mathrm{kJ/(min\,K)}$, the surface time constant is 1.60 min and the core time constant is 22.6 min. At 780 °C the linearized radiative coefficient is 212 W/(m^2 K) against 25 W/(m^2 K) for convection, so above the lithiation temperature the kiln transfers heat by radiation and the gas is present for chemistry rather than for heat.

The consequence of (11.6) is the central behavior of the plant. On a profile that ramps at R degrees per hour, the core settles roughly $0.4R$ degrees below the environment and stays there for the whole ramp. The separation is not a transient and no zone controller can remove it, because the lag is inside the solid and no controller is in that loop.

Pause. Try Exercise 11.2 before reading on.

11.3.5 Reactions

Five reduced-order reactions stand in for the synthesis, as shown in Equation (11.8).

$$\dot{X}_i = k_i(T_c)\,(1 - X_i)\,f_i(y_{\mathrm{O_2}}), \qquad k_i = k_{ref,i}\,\mathrm{e}^{-\frac{E_i}{R}\left(\frac{1}{T} - \frac{1}{T_{ref,i}}\right)} \tag{11.8}$$

where X_1 is dehydration, X_2 the decomposition of the transition-metal hydroxide, X_3 the transformation of lithium hydroxide, X_4 oxidation and lithiation, and X_5 layered ordering. Rates are written against a reference temperature so that each constant in Table 11.2 is a rate at a temperature rather than a bare pre-exponential. Kinetics run on the core temperature, which is what makes the core the variable of interest. The oxygen factors are saturating, as shown in Equation (11.9), because more oxygen stops buying anything once the surface is covered.

$$f_4 = \frac{y_{\mathrm{O_2}}}{K_{\mathrm{O_2}} + y_{\mathrm{O_2}}}, \qquad f_5 = \frac{y_{\mathrm{O_2}}}{K_{\mathrm{O_2},s} + y_{\mathrm{O_2}}}\,X_4 \tag{11.9}$$

Moving from air to 87 % oxygen raises f_5 from 0.46 to 0.78, while moving on from 87 % to 99 % adds three percent more. The dependence of f_5 on X_4 is what makes an under-lithiated brick unable to order however long it is held. The reaction windows are calibrated so that each of the first four is at least fifty times faster at the top of its window than at the bottom, which makes it a switch that completes inside one zone. The fifth is deliberately a slope, eighteenfold over 100 °C, because layered ordering is the reaction that runs out of time when the line speeds up and a switch cannot do that.

11.3.6 Quality Accumulators

Conversion alone does not decide whether material is saleable. Four further states accumulate along the path of each parcel, as shown in Equation (11.10).

$$\begin{aligned}
\dot{D} &= k_D\,[\max(0,\, T_s - T_{dam})]^2 \\
\dot{G} &= k_G\,[\max(0,\, |T_s - T_c| - \Delta T_{allow})]^2 \quad \text{for } T_c > T_g \\
\dot{C} &= X_5\, g(T_s)\,(k_{\mathrm{CO_2}} y_{\mathrm{CO_2}} + k_{\mathrm{H_2O}} y_{\mathrm{H_2O}}) \\
\dot{E} &= y_{\mathrm{O_2}}\,\dot{X}_5
\end{aligned} \tag{11.10}$$

where D is overfire damage, G gradient stress accumulated only where the core is hot enough for a gradient to cost product, C surface contamination and E the oxygen exposure weighted by

ordering progress. The contamination sensitivity $g(T_s) = [1 + \exp((T_s - 420)/60)]^{-1}$ switches on as the material cools, which puts the carbonate and hydroxide pickup in the cooling section [16, 17] rather than in the firing zones. The quality index of Equation (11.11) combines them.

$$\begin{aligned} Q = 100 &- w_4(1 - X_4)^2 - w_5(1 - X_5)^2 - w_D D - w_G G \\ &- w_O \left[\max(0, E_{min} - 100E/X_5)\right]^2 - w_C C \end{aligned} \tag{11.11}$$

Material is saleable when $Q \geq 95$, $X_4 \geq 0.99$ and $X_5 \geq 0.97$. The index is a process-quality proxy assembled from quantities this model knows about. It is not a prediction of cell capacity, first-cycle efficiency or cycle life, and the specification numbers on it are teaching defaults.

11.3.7 Zone Energy and Atmosphere Balances

Each zone integrates the energy balance of Equation (11.12).

$$\begin{aligned} C_z \frac{\mathrm{d}T_{z,j}}{\mathrm{d}t} = \eta P_{max} u_j &- UA_j (T_{z,j} - T_a) - Q_{b,j} \\ &- (F_z + F_{lk}) C_{p,g} (T_{z,j} - T_a) \\ &+ f_{rec} F_{in,j} C_{p,g} (T_{z,j+1} - T_{z,j}) - Q_{ax,j} \end{aligned} \tag{11.12}$$

where $Q_{b,j} = \sum_k w_{k,j} q_k$ is the heat drawn by every parcel coupled to the zone, F_z is the purge into it, $F_{in,j}$ is the counter-current gas arriving from the zone downstream, $f_{rec} = 0.25$ is the fraction of that enthalpy that equilibrates with the zone rather than passing through the freeboard, and $Q_{ax,j}$ is a small conductive exchange with the neighbors.

Three gas fractions are integrated per zone, as shown in Equation (11.13).

$$\begin{aligned} n_g \frac{\mathrm{d}y_{s,j}}{\mathrm{d}t} = F_z (y_{s,in} - y_{s,j}) &+ F_{in,j} (y_{s,j+1} - y_{s,j}) \\ &+ G_{s,j} - y_{s,j} \textstyle\sum_s G_{s,j} + F_{lk} (y_{s,a} - y_{s,j}) \end{aligned} \tag{11.13}$$

where $G_{s,j}$ is the generation of species s by the reactions in zone j, being water from reactions 1 to 4, carbon dioxide from residual carbonate, and a negative term for the oxygen taken up by lithiation. The three gas sections each vent separately, so $F_{in,j}$ is zero at a section boundary. With $n_g = 90\,\mathrm{mol}$ per zone and $30\,\mathrm{m^3/h}$ (normal) of purge, the atmosphere settles in under a minute, which makes it the fast subsystem inside a thirty-hour process.

The kiln pressure answers a flow imbalance in well under a second, three orders of magnitude faster than anything else in the model. It is solved algebraically from the flow balance and then lagged by the fan drive, the damper and the transmitter, as shown in Equation (11.14).

$$\begin{aligned} \tau_P \frac{\mathrm{d}P}{\mathrm{d}t} &= P^* - P \\ k_d u_{ex} (P^* + P_{fan}) &= \textstyle\sum_j F_{z,j} + \sum_j G_j + F_{lk} \end{aligned} \tag{11.14}$$

with $F_{lk} = k_L \max(0, -P^*)$. The branch matters: once the algebraic solution goes negative the kiln is pulling room air in through its seals, and the leakage term enters the balance it is the solution of. A kiln below ambient dilutes the oxygen it is paying for and carries ambient moisture to the cooling product, which is why the pressure loop belongs in the quality discussion.

11.3.8 Parameters and Numerics

Table 11.2 lists the parameters that set the behavior discussed here. The state vector has 532 entries: ten zone temperatures, ten heater powers and thirty gas fractions, the conveyor phase and the pressure, and twelve states for each of the forty parcels. Integration is fixed-step fourth-order Runge-Kutta at 0.15 min with a 1.5 min controller scan, and the engine of Section 1.6.1 makes every run repeat exactly.

Table 11.2 Model parameters. Visible parameters are shown in the application and adjustable ones may be changed by the user.

Symbol	Meaning	Value	Status
L_K	heated kiln length	40 m	fixed
N_Z	thermal zones	10	fixed
N_C	material parcels	40	fixed
N_L	parallel lanes	8	adjustable
$L \times W \times H$	brick dimensions	$0.30 \times 0.15 \times 0.10$ m	adjustable
p_b	brick pitch on the belt	0.34 m	adjustable
ρ_b	compacted density	2500 kg/m^3	adjustable
ρ_{loose}	loose blend density	833 kg/m^3	adjustable
C_p	solids heat capacity	0.90 kJ/(kg K)	adjustable
f_s	surface mass fraction	0.35	adjustable
h	gas convection	1.50 kJ/(min m^2 K)	adjustable
ε	brick emissivity	0.80	adjustable
k_{eff}	effective conductivity	0.081 kJ/(min m K)	adjustable
C_z	zone thermal mass	1850 kJ/K	adjustable
UA_z	base zone loss	0.95 kJ/(min K)	adjustable
P_{max}	zone heater rating	6000 kJ/min	adjustable
η	heater coupling	0.92	adjustable
$k_{ref,1}$	dehydration at 100 °C	0.050/min	visible
$k_{ref,4}$	lithiation at 520 °C	0.020/min	visible
$k_{ref,5}$	ordering at 780 °C	0.0145/min	visible
E_5/R	ordering activation	30 000 K	visible
$\Delta H_{1..4}$	reaction enthalpies	267, 134, 78, 47 kJ/kg	visible
T_{dam}	overfire threshold	805 °C	adjustable
ΔT_{allow}	allowable gradient	25 °C	adjustable
T_g	gradient matters above	600 °C	adjustable
n_g	gas hold-up per zone	90 mol	adjustable
τ_P	draft response	3.0 min	adjustable
θ_{lab}	assay delay	360 min	adjustable
Δt	integration step	0.15 min	fixed
Δt_c	controller scan	1.5 min	fixed

The design recipe asks the product to follow 25, 120, 250, 400, 525, 675, 770, 780, 780, 600 and 350 °C at the ten zone boundaries. The zone setpoints that deliver it are not those numbers. They are found by inverting the Lagrangian march so that the brick core meets the recipe at the middle of each zone, and they are 130, 310, 355, 525, 625, 745, 782, 781, 672 and 420 °C. Zone 2 runs 125 °C above its mid-zone product target of 185 °C because the dehydration endotherm is 267 kJ/kg and all of it lands there, and zone 3 then needs little because the endotherm has finished and the counter-current exhaust is doing the work.

11.3.9 Assumptions

Each brick is two thermal nodes joined by one conductance. A real compact has a continuous internal profile, a conductivity that rises as the particles sinter and the porosity closes, and a gas permeability

that decides how quickly oxygen reaches the middle. The single fitted conductance is the largest idealization here, and the model is least trustworthy in the thick, dense, fast-heated case that is also the most interesting one.

Oxygen reaches the core instantly. There is no intra-brick gas diffusion, so a brick too dense to breathe is represented only through its thermal lag. In a real compacted charge the oxygen gradient through the thickness can matter as much as the temperature gradient, and it is the main reason industrial charges are shallow.

Parcel mass is constant through the firing. Water and carbon dioxide leave and oxygen is taken up, which is a 28 % mass loss, but the parcel keeps its green mass in the thermal calculation, which overstates the late-stage heat capacity by roughly a quarter.

Five lumped reactions stand in for the whole synthesis, with constant enthalpies and no dependence on the lithium to transition-metal ratio. The chemistry is nickel-rich NMC and nothing else, with no dopants and no coatings. The gas in each zone is perfectly mixed and axial transport is a directed counter-current purge plus one dispersion coefficient. Cooling below about 420 °C happens outside the modeled kiln, so surface contamination picked up after the discharge is not counted.

11.4 Controller Design

Five control layers are implemented, each adding one element to the one before it. The progression is the argument of this chapter: ten competent zone loops do not control the material, a surface cascade is better and still insufficient, and only an estimator that carries the two-node model reaches the variable that decides the product.

11.4.1 Velocity Form PID Algorithm

All thirteen loops run the velocity-form algorithm of Section 1.6.2, written in this chapter's symbols in Equations (11.15) and (11.16).

$$
\begin{aligned}
e_k &= a\,(\mathrm{SP}_k - \mathrm{PV}_k) \\
\Delta u_k^{P} &= K_c\,(e_k - e_{k-1}) \\
\Delta u_k^{I} &= \frac{K_c}{\tau_I}\,e_k\,\Delta t_c \\
\Delta u_k^{D} &= -\,a\,K_c\,\tau_D\,\frac{\mathrm{PV}_k^{f} - 2\,\mathrm{PV}_{k-1}^{f} + \mathrm{PV}_{k-2}^{f}}{\Delta t_c}
\end{aligned}
\tag{11.15, 11.16}
$$

where $a = \pm 1$ sets the controller action and PV^{f} is the measurement filtered for the derivative path (a 1 min first-order filter on the zone loops, whose derivative time is zero as shipped). The zone and oxygen loops use $a = +1$ and are reverse acting, because both process gains are positive. The pressure loop uses $a = -1$ and is direct acting, because opening the damper lowers the pressure. The demand is clipped to the actuator span, and back-calculation [18] corrects the integral alone, as shown in Equation (11.17).

$$
\begin{aligned}
s_k &= s_{k-1} + \Delta u_k^{P} + \Delta u_k^{D} \\
c_k &= s_k + I_{k-1} \\
u_k &= \min(u_{max},\ \max(u_{min},\ c_k)) \\
I_k &= I_{k-1} + \Delta u_k^{I} + \frac{\Delta t_c}{\tau_t}\,(u_k - c_k)
\end{aligned}
\tag{11.17}
$$

The symbols map onto Equations (1.15) to (1.18) as $s_k = S_k$ and $c_k = v_k$ with no output bias, and the tracking time is $\tau_t = T_t = \tau_I$. At the zone tuning used below each scan therefore removes 6 % of the clipped excess. In the architectures that carry a feedforward the correction of Equation (11.20) is added to u_k after this clip and the sum is clipped to the heater span again, a limit the integral does not see. Manual operation and bumpless transfer are those of Section 1.6.2.

11.4.2 Zone Temperature Loops and Their Identification

Stepping the zone 7 heater from 45.5 to 55.5 % in manual, with the other nine zones in automatic, raises that zone by 9.0 °C within four hours. About 0.4 °C of the rise is drift that the same run shows without the step, because 45.5 % is slightly above the mean duty of the zone, so the step itself is worth 8.5 °C. A least-squares fit of the first-order plus dead-time form of Equation (11.18) to the difference between the two runs over the first 600 min, timed from the controller scan at which the step reaches the heater, returns the constants shown with it.

$$G_z(s) = \frac{K_p\, \mathrm{e}^{-\theta_p s}}{\tau_p s + 1} \qquad K_p = 0.86\,^{\circ}\mathrm{C}/\%, \quad \tau_p = 34.8\,\mathrm{min}, \quad \theta_p < 0.5\,\mathrm{min} \tag{11.18}$$

The gain is small for a heater rated at 100 kW, and the reason is worth reading off the energy balance. The zone does not keep the extra heat. It passes into the bricks, the bricks carry it into zone 8, and the zone 8 controller answers by turning its own heater down. What survives in zone 7 is the extra wall loss, the extra purge enthalpy and a little conduction to the neighbors. The same step moves the brick core by 5.5 °C, reaching 63 % of that change after 63 min, so the product gain is 0.55 °C/% and the product lag is nearly twice the measured one.

The path from heater to zone carries no transport delay, only a 0.6 min heater lag, and the thermocouple adds a 0.9 min lag of its own. The fitted dead time is therefore zero on the zone temperature and about 1 min on the thermocouple reading, a fitted dead time that is not transport in the sense of Section 1.4.2, and the SIMC rule of Equation (11.19) [19] cannot take $\tau_c = \theta_p$ as it would on a plant with real delay.

$$K_c = \frac{\tau_p}{K_p(\tau_c + \theta_p)}, \qquad \tau_I = \min(\tau_p,\ 4(\tau_c + \theta_p)) \tag{11.19}$$

The closed-loop speed is instead limited by the 1.5 min controller scan and by the interaction between neighboring zones, and the application uses $K_c = 4.0\,\%/^{\circ}\mathrm{C}$ with $\tau_I = 25$ min. That gain corresponds to τ_c near 10 min in (11.19), and the reset is shorter than the rule returns because the lag this loop has to remove is the zone rather than the material behind it. Against the cautious settings $K_c = 0.60$ and $\tau_I = 90$ min, an 18 °C setpoint move reaches 95 % of its final value in 22 min rather than 729 min, with 3.6 % overshoot, each response taken against the same run without the step so that the parcel ripple cancels. The core reaches 63 % of its own change in 35 min rather than 121 min, so the retuning makes the core 3.5 times faster while it makes the zone 33 times faster, because the conduction lag inside the brick is untouched by any tuning. In both cases the core moves only about 11.6 °C of the 18 °C the setpoint asked for, because zones 6 and 8 are holding their own temperatures and pulling the material back toward the old profile. Ten zone loops in one kiln are not ten independent loops. The heater clips at 100 % for the first few scans of the fast response, so the tracking time matters here. Absorbing the whole clipped excess in one scan would cut the overshoot to 0.9 % and stretch the 95 % time to 39 min.

11.4.3 Throughput Feedforward

A load cell on the belt and an encoder on the conveyor together measure the mass entering the kiln before any thermocouple moves. The correction that measurement justifies is not a fraction of the zone duty, because most of a zone duty is wall loss and purge enthalpy and the radiant exchange with the bricks is set by a temperature difference rather than by a mass. What scales with the feed rate is the enthalpy the material carries out of each zone, which is the sensible heat of the temperature rise across it plus the reaction heat consumed in it, as shown in Equation (11.20).

$$u_j^{ff} = K_{ff}\, r_j \frac{100\,\dot{m}_0\,[C_p \Delta T_{c,j} + \sum_i \Delta H_i \Delta X_{i,j}]}{\eta P_{max}} \tag{11.20}$$

where $\Delta T_{c,j}$ and $\Delta X_{i,j}$ are read from the design profile across zone j, and r_j is the fractional change of the measured feed rate from its value at the start of the run, the feed the kiln was prefilled with and the profile read at (the design feed in every scenario except the supervisory one, which starts at 90 %), averaged at three points over the window in which the affected material crosses that zone, which runs from jL_z/v to $(j{+}1)L_z/v$ after the measurement. The timing is the part that matters. The transport delay from the load cell to zone 10 is 1710 min at the design speed, so a correction applied to all ten zones at once is compensating nine of them for a disturbance that has not arrived. The windows scale with $1/v$, a delay that varies with flow as in Section 1.4.4. Volume 3, Chapter 6 meets the reverse arrangement, a feedforward from an upstream measurement that replaces feedback sitting hours behind the dose.

11.4.4 Soft Sensor and the Product Cascade

The core temperature estimate is the two-node model of (11.5) and (11.6) without the reaction heat terms and with the linear mean of the two zone temperatures as the radiative environment, marched forward on the *measured* zone temperatures with the estimator's own conductance $\hat{K}_{sc}$ and corrected at the discharge by the exit pyrometer, as shown in Equation (11.21).

$$\hat{T}_{s,N_C} \leftarrow \hat{T}_{s,N_C} + L\left(T_{pyro} - \hat{T}_{s,N_C}\right) \tag{11.21}$$

with $L = 0.15$. Four properties of the estimator follow from this structure. What it adds is the line speed and the brick geometry, which no temperature loop knows. It inherits every bias in the thermocouples that feed it, so it is not an independent check on them. The correction reaches the surface node only, so the core error is almost untouched by it, which is the usual situation with a partially observed state [13] (Section 1.4.6). And the direction of a modeling error decides whether it is dangerous, because an estimator that believes the brick conducts better than it does reports a core that is too hot and the outer loop lowers the firing profile until the reported core is on target. The soft sensors of Section 1.4.8 are corrected by a laboratory bias update, and Chapter 10 holds an inferred moisture that way. This estimator has no such update from the assay.

Pause. Try Exercise 11.3 before reading on.

The outer loop compares the estimate of the material in zone 7 against a product target and trims the setpoints of zones 1 to 8, everything upstream of the cooling section, by a common bias bounded to $\pm 60\,^{\circ}\mathrm{C}$, at $K_c = 1.2\,^{\circ}\mathrm{C}/^{\circ}\mathrm{C}$ and $\tau_I = 180\,\mathrm{min}$. Two variants are provided. The surface cascade holds $\hat{T}_s$ and the core cascade holds $\hat{T}_c$, and the difference between them is the subject of Section 11.5.

11.4.5 Supervisory Optimizer

The supervisory layer owns the conveyor speed and the profile trim. Every 30 min of plant time it marches a brick through each candidate zone profile at each candidate speed using the routine that prefills the kiln, relaxes any zone whose predicted duty exceeds its heater rating toward what that heater can actually hold, and evaluates the constrained problem of Equation (11.22).

$$\begin{aligned} \max_{v,\ \Delta T} \quad & \dot{m}(v) \\ \text{s.t.} \quad & X_{4,f} \geq X_{4,min}, \quad X_{5,f} \geq X_{5,min} \\ & \max |T_s - T_c|_{T_c > T_g} \leq 1.5\,\Delta T_{allow} \\ & E \geq E_{min}, \qquad Q_f \geq Q_{min} + \Delta Q \\ & u_j \leq 100\,\% \ \ \forall j \end{aligned} \tag{11.22}$$

The search is a coarse grid over four profile trims and twelve speeds followed by a two-percent refinement, and the constraint that stops the refinement is reported to the operator as the active limit. When no candidate clears the specification the layer takes the point with the best predicted quality and names the binding constraint, because a constraint the conveyor cannot reach, such as an oxygen

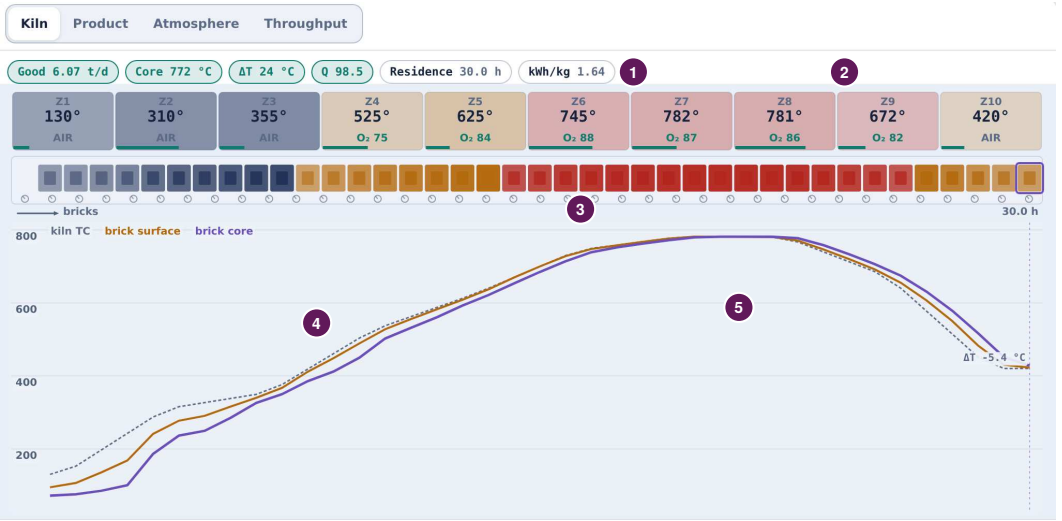


Figure 11.2 The Kiln view of the application at the design point (scenario 5) after 30 h, one residence time, with all ten zone loops in automatic, cropped from the full screen. Callouts: (1) the product tiles, (2) the ten zone tiles with their setpoints and firing-section oxygen, (3) the strip of brick parcels on the belt, (4) the dehydration ramp and (5) the high-temperature hold. The three curves drawn along the kiln are the zone temperature the controllers hold (dotted), the brick surface and the brick core. They coincide through the high-temperature hold and separate wherever the profile ramps, which is the behavior the application exists to show. At this instant the zone 7 trend, cropped from this view, reads 781.9 °C against a 782 °C setpoint while the brick core in that zone is at 772.0 °C.

supply restriction, does not improve by running slower. The core cascade stays in service beneath the layer, which adds its trim to the cascade output and clips the sum to $\pm 60\,^{\circ}\mathrm{C}$, and the conveyor drive ramps toward the chosen speed at 1.2 % of design per minute.

This is a steady-state economic optimization over a dynamic model, evaluated on a slow schedule and handed down to the regulatory layer as setpoints. It is deliberately not a receding-horizon quadratic program of the kind Section 1.6.3 describes, it carries no explicit disturbance model and no state estimator of its own, and it assumes the zone profile it is given will still be there thirty hours later. The supervisor of Chapter 5 has the same structure, a grid search on a forecast from a thermal-history estimator instead of a loop closed on the forecast.

11.5 Results

All results are measured on the application at its shipped settings. Each case starts by selecting its scenario and changing any setting before the run begins, which gives the same run as that setting carried through a Reset (Section 1.6.1), and each run is carried past one full residence time so that the material leaving the kiln reflects the condition being tested. The application ships fifteen scenarios, from open-loop observation through identification and tuning to a graded challenge, and Section 1.6.4 describes how each is credited. The design point (scenario 5) produces 6.07 t/d of cathode active material at a quality index of 98.6, an exit ordering of 0.9862, a worst firing-region gradient of 25.5 °C against an allowance of 25, a busiest heater at 72 % in zone 8, and 1.602 kW h/kg of heater energy per kilogram of product. The screenshot in Figure 11.2 shows that condition.

Table 11.3 Design profile. Zone setpoints, heater loading, firing-section oxygen, and the brick surface and core temperatures at each zone center.

Zone	T_z^{SP} (°C)	u (%)	y_{O_2} (%)	T_s (°C)	T_c (°C)
1	130	17	10	113	78
2	310	63	11	241	194
3	355	25	17	361	336
4	525	45	75	504	474
5	625	24	84	625	607
6	745	64	88	730	719
7	782	45	87	775	772
8	781	72	86	766	770
9	672	28	82	663	681
10	420	22	30	481	503

11.5.1 The Separation Between Kiln and Product

Table 11.3 lists the design profile. Through zones 7 and 8, where the recipe holds flat, the core sits within 11 °C of the thermocouple and within 5 °C of the surface. Through the dehydration and annealing ramps the separation reaches 71 °C, with the dehydration endotherm pulling the core down while the surface stays on the profile. No zone controller is at fault anywhere in the table, and every zone is on setpoint throughout.

The sign of the separation reverses in the cooling section, where the surface leads the core downward. At zone 9 the surface is 18 °C below the core and at zone 10 it is 22 °C below. That reversal is a useful check on the two-node structure, because a model that produced a fixed offset rather than a lag would not show it.

11.5.2 Case Studies

Table 11.4 collects the measured outcomes. Zone 7 integrated absolute error is taken against the *true* zone temperature over the 1800 min following each event, which is one residence time, and from the start of the run where the condition applies from the start (cases A, D and I). Case B is scenario 7 with its cautious tuning, C, E and F are scenarios 9, 10 and 6, G and H are scenario 12 on the two cascades, and D and I are scenario 5 with the oxygen supply or the supervisory layer changed before the run. Figure 11.3 draws the exit ordering, the quality index and the good production rate of each case.

Case B, a heavier load. Ten percent denser bricks are ten percent more tonnes, ten percent more thermal mass and ten percent more reaction endotherm, and the load arrives as a wave that takes a full residence time to reach the exit. With the cautious tuning, adding the feedforward of (11.20) reduces the error summed over all ten zones in the 1800 min after the change from 4641 to 3424 °C min, a reduction of 26 %. With the SIMC tuning it is worth almost nothing (1846 against 1832 °C min), because those loops already hold every zone in the kiln within 0.52 °C, the residual ripple of zone 10 in the undisturbed kiln, and there is nothing left for a feedforward to remove. A feedforward earns its keep against the feedback it is added to rather than against the disturbance.

Case C, a wet feed. Fifty percent more free moisture is a larger endotherm concentrated in the first three zones. The zone loops take it, holding every thermocouple within 0.52 °C, and the material does not: the worst surface-to-core difference anywhere in the kiln rises from 71 to 87 °C and the specific energy rises from 1.602 to 1.632 kW h/kg. A mass feedforward is blind to this disturbance by construction, because moisture does not change the mass on the belt.

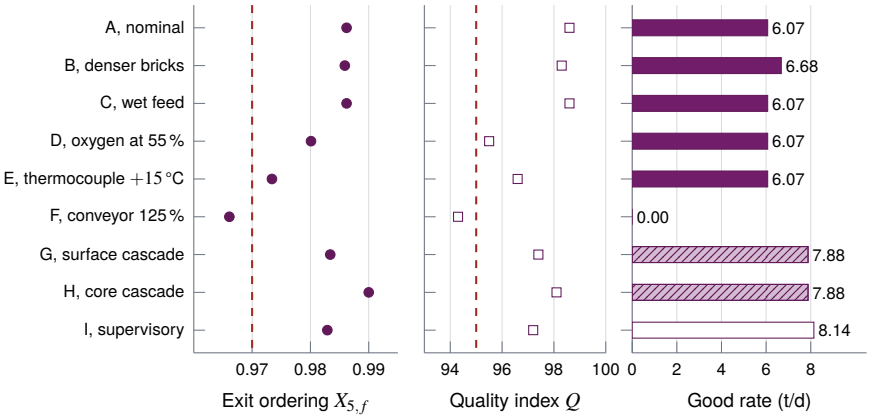


Figure 11.3 The case studies of Table 11.4: the exit ordering (left, dashed line at the 0.970 minimum), the quality index (middle, dashed line at the minimum of 95) and the good production rate (right). Dark bars are the zone loops, hatched bars the two cascades and the white bar the supervisory layer. Notice that in cases D and E every zone reading stays on its setpoint while the ordering falls, and that at the same 7.88 t/d the core cascade orders the material further than the surface cascade.

Table 11.4 Measured case studies. Zone 7 IAE and peak error are against the true zone temperature over the 1800 min after the case's first event (from $t = 0$ for A, D and I), evaluated at the 0.15 min integration step. Exit values are those of the parcel at the discharge at the end of the run. Q uses that same parcel throughout. The app tile instead averages the last sixteen scored exits.

Case	Condition	Zone 7 IAE (°C min)	Peak $\lvert e \rvert$ (°C)	$X_{5,f}$	Worst ΔT (°C)	Q	Good rate (t/d)	SEC (kW h/kg)
A	nominal, 10 zone loops	167	0.27	0.9862	25.5	98.6	6.07	1.602
B	brick density +10 %	262	0.82	0.9859	26.2	98.3	6.68	1.576
C	feed moisture 1.5×	167	0.17	0.9862	24.2	98.6	6.07	1.632
D	oxygen supply at 55 %	167	0.27	0.9801	25.5	95.5	6.07	1.602
E	zone 7 thermocouple +15 °C	26938	15.90	0.9734	24.3	96.6	6.07	1.614
F	conveyor at 125 %	140	0.24	0.9661	31.4	94.3	0.00	1.356
G	surface cascade at 118 %	349	0.57	0.9834	32.8	97.4	7.88	1.409
H	core cascade at 118 %	276	0.45	0.9900	32.9	98.1	7.88	1.417
I	supervisory optimizer	531	19.54	0.9829	31.5	97.2	8.14	1.300

Case D, an atmosphere fault. Restricting the oxygen supply to 55 % of capacity saturates the blend command and lowers the firing-section oxygen. No temperature in the kiln moves. The exit ordering falls from 0.9862 to 0.9801 and the quality index from 98.6 to 95.5, entirely through the oxygen factor f_5 of (11.9).

Case E, a biased thermocouple. A sheath that reads 15 °C high produces the most instructive row in the table. The controller holds the *reading* at setpoint, so the measured error is near zero while

Table 11.5 Conveyor speed against product and production. Good production is the gross rate multiplied by the fraction that meets the specification.

v (%)	τ_K (h)	$X_{5,f}$	Q	Gross (t/d)	Good (t/d)	SEC (kWh/kg)
90	33.33	0.9916	98.86	5.47	5.47	1.754
100	30.00	0.9862	98.62	6.07	6.07	1.602
110	27.27	0.9792	97.55	6.68	6.68	1.494
115	26.09	0.9752	96.80	6.98	6.98	1.440
120	25.00	0.9708	95.58	7.29	7.29	1.404
121	24.79	0.9699	95.34	7.35	0.00	1.394
125	24.00	0.9661	94.27	7.59	0.00	1.358
130	23.08	0.9610	92.62	7.90	0.00	1.316
140	21.43	0.9500	88.03	8.50	0.00	1.252

the error against the true zone temperature integrates to 26 938 °C min over one residence time, 161 times the nominal case over a window of the same length. The exit ordering falls to 0.9734 and the quality index to 96.6. Nothing inside the loop can find this, and the evidence has to come from the exit pyrometer, a second thermocouple, or the assay six hours downstream.

> **TRY IT IN THE APP** **10 · A Thermocouple That Reads 15 °C High**
>
> Load the scenario and press Run. After the thermocouple fault fires, watch the zone 7 strip on the Kiln tab: the dotted TT-107 reading stays on its setpoint while the true zone temperature sits below it. Then open the Product tab as the cold-fired material reaches the exit, where the ordering falls to 0.9734 and the quality index to 96.6.

Cases G and H, two cascades. At 118 % line speed both cascades deliver the same 7.88 t/d, and they do not deliver the same material. The surface cascade reaches an exit ordering of 0.9834 and a quality index of 97.4, while the core cascade reaches 0.9900 and 98.1 for 0.6 % more energy. The surface loop is not mistuned. It is holding the variable it was asked to hold, and the surface-to-core difference is not a fixed offset, so holding the surface does not hold the core. A cascade rejects the disturbances that enter inside its inner measurement, the rule that Volume 3, Chapter 2 demonstrates on a tank, and denser bricks and a faster line both act inside the brick, behind the surface.

> **TRY IT IN THE APP** **12 · A Surface Cascade, and Why It Is Not Enough**
>
> Run the full pass on the surface cascade, then reset, switch to the core cascade and run it again. Both runs end at 7.88 t/d. Compare the ordering at the exit on the Product tab: 0.9834 on the surface cascade and 0.9900 on the core cascade.

11.5.3 Throughput and the Active Constraint

Table 11.5 sweeps the conveyor speed with the recipe unchanged. Gross production rises in direct proportion and the specific energy falls, from 1.754 kW h/kg at 90 % to 1.252 kW h/kg at 140 %, because the fixed losses are spread over more kilograms. Good production, which is the gross rate multiplied by the fraction that meets the specification, has an interior maximum of 7.29 t/d at 120 % and falls to zero at 121, where the exit ordering crosses its 0.970 minimum.

Four constraints could have stopped the line and only one does. The heaters never saturate, the busiest going from 69 % to 76 % across the whole sweep, because the mass in the kiln does not change with line speed and only the required heating rate does. The cooling section is never limiting.

The oxygen exposure is unaffected by speed. What binds is the layered ordering reaction running out of time, with the surface-to-core gradient close behind it. That is the connection the application is built to make, because the capacity of the most expensive machine in the plant turns out to be set by a reaction rate in the middle of a brick.

> ✦ DID YOU KNOW? **One Percent of Line Speed Loses Everything**
>
> From the simulator: at 120 % of design speed the kiln makes 7.29 t/d of good product, its best. At 121 % the exit ordering is 0.9699, just under the 0.970 minimum, and good production is zero (Table 11.5). The specification is a cliff, not a slope.

The supervisory layer of (11.22) does better than any fixed speed, because it buys the lost ordering back with the profile trim before it spends the residence time. Chosen before the run at the design point, it moves the line to 134 % of design speed on its first execution at $t = 0$ and raises the zone 7 setpoint by 19.6 °C at the same instant, 10 °C of trim of its own and 9.6 °C from the proportional action of the core cascade on its first scan, which is the peak error of case I in Table 11.4. Zone 7 is back within 1 °C of its setpoint for good after 55 min. The layer then produces 8.14 t/d of saleable material at a quality index of 97.2 and 1.300 kW h/kg. Against the design point that is 34 % more good production for 19 % less energy per kilogram, and against the best fixed-speed operating point it is 12 % more.

11.5.4 The Graded Challenge

The graded challenge, scenario 15, adds a density change, a wet feed and a derated heater bank to a kiln that starts on the cautious zone loops at design speed. It is judged from 400 to 3600 min: zone 7 must stay within ± 3 °C of its setpoint and good production must average at least 7.4 t/d, with the model parameters and disturbances as given. Changing a model parameter or a disturbance voids the attempt. With the shipped settings the worst zone 7 error over the scored window is 2.20 °C, inside the band, but good production averages 6.68 t/d, 0.72 t/d short of the target. The supervisory layer with the SIMC zone tuning raises the average to 8.15 t/d, a gain of 22 %, with a worst error of 0.84 °C, which passes with 0.75 t/d and 2.2 °C to spare, while the specific energy at the end of the 60 h run falls from 1.610 to 1.381 kW h/kg. One change is enough. The conveyor alone at 111 to 116 % on the loops as delivered passes with 7.42 to 7.68 t/d and a worst error near 2.3 °C, while 117 % and faster send the denser, wetter material off specification.

11.6 Technology in Practice

What Measures It

Every zone of the kiln is read by a sheathed thermocouple, and the soft sensor of Section 11.4 is marched on those ten readings. A thermocouple ages in service, and its error stays hidden until the element is taken out and checked.

> TECHNOLOGY **Sensor: A Zone Thermocouple That Drifts**
>
> A thermocouple drifts as its metals change in service, by contamination and oxidation among other causes, and the reading no longer matches the original calibration. Smaller wires and higher temperatures drift faster, and type N has been found about ten times more stable than type K at high temperature. In one set of tests type K drifted by up to about 2 % within 400 h between 1000 and 1100 °C [20]. Checking the transmitter with a simulated millivolt signal does nothing to validate the element itself [21]. On a trend a drifted zone looks perfect, which is case E.

The chapter gives each zone thermocouple a 0.9 min lag and an optional constant bias, the fault of case E. The exit pyrometer reads the brick surface at the discharge, and the laboratory assay arrives 360 min after the material has left. Neither reaches the core.

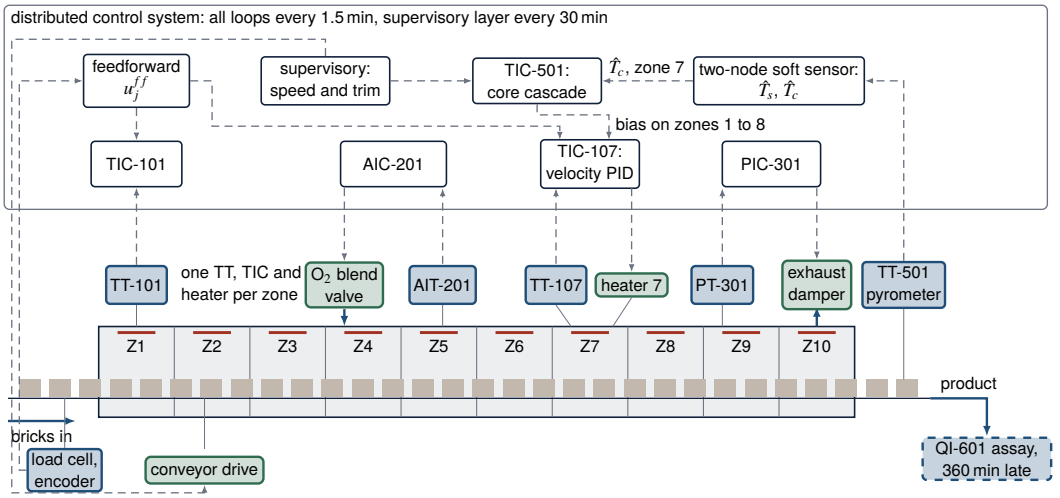


Figure 11.4 The loops of the kiln on plant hardware. Each zone has a thermocouple, a velocity-form PID loop and a heater (zones 1 and 7 drawn), and a feedforward from the load cell and encoder adds to the heater demands as the material reaches each zone. AIC-201 holds the firing-section oxygen with the blend valve and PIC-301 the kiln pressure with the exhaust damper. The soft sensor, marched on the zone readings (lines not drawn) and corrected by the exit pyrometer TT-501, feeds the core cascade TIC-501, which biases the setpoints of zones 1 to 8, and the supervisory layer sets the conveyor speed and a profile trim. Notice that no line reaches the brick core, and that the assay QI-601 corrects nothing.

What Moves It

The zone heaters move the zone temperatures, the oxygen share of the gas blend moves the firing-section atmosphere, the exhaust damper moves the kiln pressure and the conveyor drive moves the residence time. The heater is the element every zone loop acts on, and the model's 100 kW rating is the limit that the supervisory layer relaxes a profile toward.

> **TECHNOLOGY Final Element: Resistance Heaters on a Pulsed Output**
>
> In indirect resistance heating an element of a high-resistance material such as silicon carbide or nickel chrome heats the load by radiation, convection or conduction. Heaters that rely on convection are used mainly below about 1250 °F, and those that radiate at higher temperatures. Such heating is precisely controlled and easily automated [22]. An element that can only be switched fully on or off is driven by a time-proportioned output, a pulse train whose duty cycle follows the controller's demand between 0 % and 100 % [21]. The model's heater follows its command through a 0.6 min lag and saturates at its rating.

Where the Controller Runs

Loops like these run in a distributed control system. It places a supervisory level of control over the field controllers, nests or cascades loops so that one loop sets another's set point, and runs with cycle times from milliseconds to minutes [23]. A 2003 survey of predictive control draws the usual hierarchy: basic loops about every second, dynamic constraint control about every minute, and above them a local optimizer, about every hour, that computes an optimal economic steady state and passes it down [24]. Here every loop, the core cascade among them, runs on the 1.5 min controller scan, and the supervisory layer of Equation (11.22) runs every 30 min as such a local optimizer. Each loop is the velocity-form PID of Equation (11.16) as one function block. Figure 11.4 draws the loops on field devices.

What Is Modernizing It

Three developments bear on this kiln. The first is the soft sensor. A 2013 review of industrial soft sensors prefers a first-principles model where one is available with enough accuracy at reasonable modeling effort and computing load, and a survey it reports found the maintenance of models to be the most critical issue in using them [25]. The two-node estimator is such a model, and its conductance is what has to be maintained. The second is measurement. A 2015 sourcebook on process heating notes that emerging technologies can now measure feedstock and melts in real time and that advanced process control lets a heating system be predictive instead of reactive [22]. The third is the sensor itself, where calibration in place, the subject of the first open challenge, would let a drifting zone element be found without taking it out.

> **IN PRACTICE** **Hold the Kiln Slightly Above the Room**
>
> With time most furnaces develop cracks and openings around doors, joints and hearth seals, and a negative pressure draws cold air in through them. A furnace pressure controller reads a pressure gauge in the chamber and regulates the draft fan speed or a damper to hold a slightly positive pressure. Controlled-atmosphere furnaces require positive pressure and special pressure controllers, and steady pressure helps keep the temperature uniform [22]. The chapter's pressure loop does this with the exhaust damper, and below ambient the model's seals leak room air in.

11.7 Limitations

The two-node brick is the limiting idealization. A compact fired from ambient to 780 °C develops an internal profile with more structure than two nodes can carry, its effective conductivity rises as the particles sinter, and the model treats that conductivity as a constant fitted to reproduce a 22.6 min core lag. The application is therefore evidence about the *structure* of the control problem and not about the magnitude of the gradient in any particular brick.

Intra-brick oxygen transport is absent. A dense compact can be oxygen-starved in the middle while the surrounding atmosphere is rich, and that mechanism is the main reason industrial charges are shallow. In this model a brick too dense to breathe shows only a thermal lag, so the density disturbance understates what compaction costs.

The quality index is a process proxy. It is assembled from conversion, overfire exposure, thermal gradient, oxygen exposure and surface contamination, which are the quantities the model knows about, and it says nothing about particle size distribution, crystallite size, cation mixing measured by diffraction, residual lithium by titration, or any quantity an electrochemical cell would report. The specification thresholds are teaching defaults.

The supervisory layer is a steady-state optimization on a slow schedule rather than a receding-horizon controller. It assumes the zone profile it is handed will still be present when the material it is deciding about reaches the discharge thirty hours later, which is exactly the assumption a real implementation would have to relax.

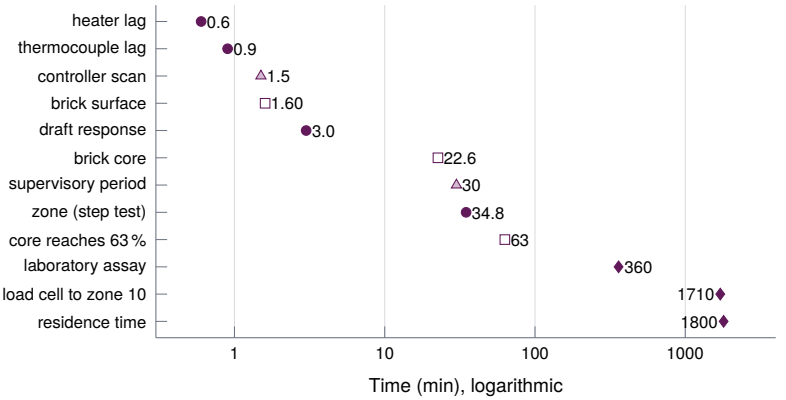


Figure 11.5 The time scales of the kiln, each as the chapter states it. Filled circles are instruments, actuators and the zone, open squares the brick, triangles the control schedule and diamonds the delays of transport and of the laboratory. Notice that the zone loops act on the left of the chart and the product is decided on the right, across more than three decades of time.

> **OPEN CHALLENGE** **A Thermocouple That Reports Its Own Drift**
>
> Unless a thermocouple is removed from time to time for recalibration, nothing during its use shows whether its output is still within specification. Recent work has explored calibrating it in place, against the melting points of reference materials built into the probe or by Johnson noise thermometry [20]. In this chapter a biased zone 7 thermocouple is invisible to its loop and to the soft sensor that runs on it, and only the exit pyrometer, a second element or the assay can find it. A zone element that checks itself in service would close that gap.

11.8 Discussion

The results rest on a separation of time scales between a 1.6 min surface node, a 22.6 min core, a 34.8 min zone and a 30 h transport delay. Figure 11.5 sets these beside the other lags, periods and delays of the chapter. The results in Table 11.4 separate two ideas that are easy to conflate. Cases C, D and E all leave the regulatory layer looking excellent and the product measurably worse, and in each the fault is visible only outside the loop that caused it. That is the generic situation of a plant whose controlled variable is inferred, and it is the reason the soft-sensor literature treats the estimator and the controller as one design rather than two [13].

The second idea is that the estimate is not free. Cases G and H differ by 0.7 points of quality index and 0.0065 of exit ordering, and the better of the two is the one built on a state that is computed rather than sensed. An estimator that believes the brick conducts better than it does reports a core that is too hot, and the outer loop responds by lowering the firing profile until the reported error is zero, which leaves the true core cold with no error visible anywhere in the control system. The application exposes that failure directly by allowing the estimator conductance to be set wrong in either direction.

The throughput result generalizes past cathode kilns. Any unit that is the bottleneck of a plant and whose product quality depends on residence time has an interior maximum in saleable production, and the location of that maximum moves whenever anything about the feed, the utilities or the equipment moves. Locating it requires predicting the quality rather than measuring it, which is the same argument that put model predictive control on lime kilns and annealing furnaces [9, 11]. The model here is deliberately reduced from the computational fluid dynamics that full-scale kiln studies use [7, 12] to something that runs in a browser in real time, which is what makes it usable as a control platform rather than as a design tool.

11.9 Conclusion

This chapter studied a ten-zone cathode calcination kiln as an interactive laboratory for controlling a state that no instrument reaches. The simulator integrates 532 states, ten zone temperatures and heater powers, thirty gas fractions, a conveyor phase and a kiln pressure, and twelve states for each of forty Lagrangian material parcels carrying two temperatures, five reaction extents and four quality accumulators.

A step test identifies the zone loop as a first-order plus dead-time plant with a gain of 0.86 °C/%, a 34.8 min time constant and negligible dead time, while the same step moves the brick core with a gain of 0.55 °C/% and nearly twice the lag. Ten zone loops tuned by SIMC hold every thermocouple within 0.52 °C of a ten percent load change and do not prevent a 15 °C thermocouple bias from costing 2.0 points of quality index, nor an oxygen restriction from costing 3.1, nor a twenty-five percent line speed increase from taking the material off specification entirely.

A core cascade built on a two-node soft sensor reaches an exit ordering of 0.9900 against 0.9834 for the same cascade closed on the brick surface. A supervisory layer that predicts the exit quality raises saleable production from 6.07 to 8.14 t/d while lowering the specific energy from 1.602 to 1.300 kW h/kg. A fuller model would add intra-brick oxygen transport, a sintering-dependent conductivity, a receding-horizon formulation of the supervisory layer, and moving horizon estimation against the delayed assay (Section 1.4.7). The cathode kiln is a plant on which to learn to control what cannot be measured.

KEY POINTS

- The temperature that sets the reactions is in the middle of a brick, and no instrument reaches it.
- On a ramp the core settles below the environment and stays there, and no zone controller can remove the separation.
- A thermocouple 15 °C high leaves its loop looking perfect while the exit ordering falls to 0.9734.
- A core cascade on the soft sensor reaches an exit ordering of 0.9900 against 0.9834 for the same cascade on the surface.
- Good production peaks at 120 % of design speed, where the ordering reaction runs out of time.

Where else this applies. Chapter 5 runs the same kind of supervisor on a thermal-history estimate, and Chapter 10 holds an inferred quality with a laboratory bias update.

References

[1] A. Kwade, W. Haselrieder, R. Leithoff, A. Modlinger, F. Dietrich, and K. Droeder, "Current status and challenges for automotive battery production technologies," *Nature Energy*, vol. 3, no. 4, pp. 290–300, 2018.

[2] W. Li, E. M. Erickson, and A. Manthiram, "High-nickel layered oxide cathodes for lithium-based automotive batteries," *Nature Energy*, vol. 5, no. 1, pp. 26–34, 2020.

[3] Z. Ye, L. Qiu, W. Yang, Z. Wu, Y. Liu, G. Wang, Y. Song, B. Zhong, and X. Guo, "Nickel-rich layered cathode materials for lithium-ion batteries," *Chemistry – A European Journal*, vol. 27, no. 13, pp. 4249–4269, 2021.

[4] H. Zhang and J. Zhang, "An overview of modification strategies to improve $LiNi_{0.8}Co_{0.1}Mn_{0.1}O_2$ (NCM811) cathode performance for automotive lithium-ion batteries," *eTransportation*, vol. 7, p. 100105, 2021.

[5] Q. Xiong, X. Geng, Z. Liu, Y. Yang, H. Wang, P. Long, Y. Yan, H. Li, H. Zeng, S. Luchkin, Y. Lin, J. Wang, and X. He, "Resolving atmosphere-regulated defect cascades in Ni-rich layered cathodes during high-temperature synthesis," *Energy Storage Materials*, vol. 90, p. 105387, 2026.

[6] The Royal Swedish Academy of Sciences, "Scientific background on the Nobel prize in chemistry 2019: Lithium-ion batteries," The Royal Swedish Academy of Sciences, Stockholm, 9 October 2019, 2019. [Online]. Available: https://www.nobelprize.org/uploads/2019/10/advanced-chemistryprize2019.pdf

[7] Y. Dai, X. Jin, P. Zhang, P. Li, Z. Shao, M. Yang, C. Cao, and W. Du, "Numerical study on calcination of Ni-Co-Mn ternary precursors in an industrial roller hearth kiln," *Chemical Engineering Research and Design*, vol. 231, pp. 169–180, 2026.

[8] N. Yoshitani and A. Hasegawa, "Model-based control of strip temperature for the heating furnace in continuous annealing," *IEEE Transactions on Control Systems Technology*, vol. 6, no. 2, pp. 146–156, 1998.

[9] M. Niederer, S. Strommer, A. Steinboeck, and A. Kugi, "Nonlinear model predictive control of the strip temperature in an annealing furnace," *Journal of Process Control*, vol. 48, pp. 1–13, 2016.

[10] S. Strommer, M. Niederer, A. Steinboeck, and A. Kugi, "Hierarchical nonlinear optimization-based controller of a continuous strip annealing furnace," *Control Engineering Practice*, vol. 73, pp. 40–55, 2018.

[11] J. Valiquette, M. Savoie, and M. Leclerc, "Practical aspects of model predictive control implementation on an industrial lime kiln," in *1997 European Control Conference (ECC)*. IEEE, 1997, pp. 2711–2715.

[12] J. Ryan, M. Bussmann, and N. DeMartini, "CFD modelling of calcination in a rotary lime kiln," *Processes*, vol. 10, no. 8, p. 1516, 2022.

[13] P. Kadlec, B. Gabrys, and S. Strandt, "Data-driven soft sensors in the process industry," *Computers & Chemical Engineering*, vol. 33, no. 4, pp. 795–814, 2009.

[14] J. Park, R. A. Martin, J. D. Kelly, and J. D. Hedengren, "Benchmark temperature microcontroller for process dynamics and control," *Computers & Chemical Engineering*, vol. 135, p. 106736, 2020.

[15] B. W. Bequette, "Process control practice and education: Past, present and future," *Computers & Chemical Engineering*, vol. 128, pp. 538–556, 2019.

[16] W. M. Seong, Y. Kim, and A. Manthiram, "Impact of residual lithium on the adoption of high-nickel layered oxide cathodes for lithium-ion batteries," *Chemistry of Materials*, vol. 32, no. 22, pp. 9479–9489, 2020.

[17] Q. Tian, R. Song, J. Zhang, Y. Chen, C. Cui, C. Ma, M. Su, and W. Hu, "Formation mechanism and removal strategy of residual lithium compounds on nickel-rich cathode materials," *Progress in Natural Science: Materials International*, vol. 34, no. 6, pp. 1158–1166, 2024.

[18] K. J. Åström and T. Hägglund, *Advanced PID Control*. Research Triangle Park, NC: ISA – The Instrumentation, Systems, and Automation Society, 2006.

[19] S. Skogestad, "Simple analytic rules for model reduction and PID controller tuning," *Journal of Process Control*, vol. 13, no. 4, pp. 291–309, 2003.

[20] R. J. Chesser and N. D. Bull Ezell, "Thermocouple and RTD drift due to neutron irradiation and temperature for space nuclear applications: A review," *IEEE Sensors Journal*, vol. 25, no. 22, pp. 40 965–40 977, 2025.

[21] T. R. Kuphaldt, *Lessons in Industrial Instrumentation*, version 2.33 ed. Open textbook, Creative Commons Attribution 4.0 license, ibiblio.org/kuphaldt/socratic/sinst, 2024.

[22] U.S. Department of Energy, Advanced Manufacturing Office, "Improving process heating system performance: A sourcebook for industry," U.S. Department of Energy, Office of Energy Efficiency and Renewable Energy, Washington, DC, Third edition, report DOE/EE-1339, 2015, oSTI ID 1247916. [Online]. Available: https://www.osti.gov/biblio/1247916

[23] K. Stouffer, M. Pease, C. Tang, T. Zimmerman, V. Pillitteri, S. Lightman, A. Hahn, S. Saravia, A. Sherule, and M. Thompson, "Guide to operational technology (OT) security," National Institute of Standards and Technology, Gaithersburg, MD, Special Publication 800-82r3, 2023.

[24] S. J. Qin and T. A. Badgwell, "A survey of industrial model predictive control technology," *Control Engineering Practice*, vol. 11, no. 7, pp. 733–764, 2003.

[25] M. Kano and K. Fujiwara, "Virtual sensing technology in process industries: Trends and challenges revealed by recent industrial applications," *Journal of Chemical Engineering of Japan*, vol. 46, no. 1, pp. 1–17, 2013.

11.10 Exercises

11.1 ○ Concept check · 1 min

Which of the following quantities is measured on the kiln and available to a controller as the run proceeds?

(a) The brick core temperature T_c in zone 7

(b) The lithiation extent X_4 of the material at the exit

(c) The zone 7 temperature $T_{z,7}$, read by its thermocouple

(d) The quality index Q of the material leaving the kiln

11.2 Concept check · 2 min

Equation (11.6) is the energy balance on the brick core. With the reaction term left out, what sets the time constant with which the core follows its surface, and why can no zone loop shorten it?

(a) The zone thermal mass over its loss, C_z/UA_z, which a higher zone gain shortens

(b) The 1.5 min controller scan, which a faster scan of the zone loops would remove

(c) The 0.9 min thermocouple lag, which derivative action on the zone loops would cancel

(d) The ratio $m_c C_p/K_{sc}$, a property of the brick that no controller acts on

11.3 Concept check · 2 min

The zone 7 thermocouple of the kiln at its design point begins to read 15 °C high, as in scenario 10. The zone loops and the soft sensor are otherwise unchanged. Which statement is right?

(a) The zone runs about 15 °C cold, the ordering rate falls by about a third, and the evidence must come from outside the loop

(b) The zone 7 error against the reading grows at once, so the loop's own scorecard reveals the fault within the hour

(c) The soft sensor sees the core run cold, so the core cascade, if selected, restores the true core temperature

(d) The zone runs about 15 °C cold, but the ordering rate barely changes because the reaction saturates there

11.4 Theory and calculation · 5 min

The kiln of Table 11.2 carries $N_L = 8$ lanes of bricks of 0.0045 m^3 at 2500 kg/m^3, spaced 0.34 m apart along the belt. A parcel is 1 m of belt, the kiln is 40 m long in ten zones of 4 m, and the design residence time is 30.0 h.

(a) Find the brick mass, the number of bricks in a parcel and the parcel mass. *Checkpoint:* 11.25 kg, 23.5 and 264.7 kg.

(b) Find the design conveyor speed and the green feed rate. With the 28 % mass loss of the firing, estimate the product rate in tonnes a day. *Checkpoint:* 1.333 m/h, 353 kg/h and about 6.10 t/d.

(c) Repeat the residence time and the feed rate at 125 % of design speed, and find at both speeds the center of the window in which material weighed at the load cell crosses zone 10. *Checkpoint:* 24.0 h and 441 kg/h. 1710 min at design and 1368 min at 125 %.

11.5 Theory and calculation · 8 min

Use the brick data of Table 11.2: $L \times W \times H = 0.30 \times 0.15 \times 0.10$ m, $k_{eff} = 0.081$ kJ/(min m K), $C_p = 0.90$ kJ/(kg K), $f_s = 0.35$, with a parcel of $m = 264.7$ kg holding $n_b = 23.53$ bricks, an exposed area $A = 3.18$ m^2, a convection coefficient $h = 1.50$ kJ/(min m^2 K) and a linearized radiative coefficient of 212 W/(m^2 K) at 780 °C.

(a) Compute K_{sc} from Equation (11.7). *Checkpoint:* 6.86 kJ/(min K).

(b) Compute the core time constant from Equation (11.6), and the surface time constant from Equation (11.5) linearized at 780 °C with the zone and the core held fixed. Leave out the reaction terms. *Checkpoint:* 22.6 min and 1.60 min.

(c) A first-order node driven by an input that ramps at a steady rate R settles a fixed $R\tau$ behind it. Use this to recover the $0.4R$ of Section 11.3 with R in degrees per hour. The recipe falls from 780 to 600 °C across zone 9. Find R there and the surface-to-core difference $R\tau_c$ at design speed and at 125 %. *Checkpoint:* $0.40R$. 60 °C/h and 22.6 °C. 75 °C/h and 28.2 °C.

11.6 Theory and calculation · 6 min

Use the zone model of Equation (11.18) and the SIMC rule of Equation (11.19).

(a) Take $\theta_p = 0$ and $\tau_c = 10\,\text{min}$. Find K_c and τ_I and compare them with the settings the app uses. *Checkpoint:* 4.05 %/°C and 34.8 min, against 4.0 and 25 min.

(b) An engineer takes the 1 min fitted on the thermocouple reading as θ_p and sets $\tau_c = \theta_p$. Find the settings, and give two reasons from the chapter why they would not work on this kiln. *Checkpoint:* 20.2 %/°C and 8 min.

(c) The same heater step moves the core by 0.55 °C/%. Predict how far the core in zone 7 moves when the zone 7 setpoint is raised 18 °C and the zone loops hold their setpoints. *Checkpoint:* About 11.5 °C.

11.7 App challenge · 10 min

Load scenario 2 · Step one zone and identify it (MANUAL), with the default seed. Before pressing Run, set Zone 7 heater to 55.5 %. Run to 240 min at a speed of 60, which takes 4 s, and export the CSV file.

(a) From columns `z7_C` and `z7_core_C`, find the rise of the zone and of the core between the first row and the last row before 240 min, and the first row at which each has covered 63.2 % of its rise. *Checkpoint:* Zone 8.95 °C at 31.5 min, core 6.09 °C at 60.9 min, within 0.05 °C and one row.

(b) Press the reload button, change nothing, run to 240 min again and read the same two columns at the end. Find the part of each rise that the step caused, and the two gains. *Checkpoint:* Drift 0.43 and 0.58 °C. Step 8.52 and 5.50 °C, gains 0.85 and 0.55 °C/%.

(c) Repeat the 63.2 % times on the difference between the two runs and compare them with Equation (11.18). *Checkpoint:* 34.6 min for the zone and 63.0 min for the core.

11.8 App challenge · 8 min

Load scenario 6 · The kiln is on setpoint and the core is not, with the default seed. The conveyor steps from 100 to 125 % at 30 min. Run to 1800 min at a speed of 120, which takes 15 s, and export the CSV file.

(a) Find the largest deviation of `z7_C` from `z7_sp_C` after 30 min. *Checkpoint:* 0.24 °C, within 0.02 °C.

(b) At 1800 min read the tiles Ordering at the exit, CAM quality index and Good production, and the column `gross_tpd`. *Checkpoint:* 96.6 %, 94.2, 0.00 t/d and 7.59 t/d.

(c) Find the first row with `quality_exit` below 95. Material that entered after the speed change needs 24 h to reach the exit. Explain why the exit fails much sooner. *Checkpoint:* 692 min, within one row. That parcel was 21.6 m from the inlet at the step, ahead of the hold.

11.9 App challenge · 9 min

Load scenario 12 · A surface cascade, and why it is not enough, with the default seed. The bricks become 10 % denser at 60 min and the conveyor steps to 118 % at 900 min. Run each case to 3600 min at a speed of 120, which takes 30 s, and export the CSV file.

(a) Run the scenario as loaded, on + Surface cascade. Read the tiles Ordering at the exit and CAM quality index, and the columns `profile_bias_C`, `z7_surf_C` and `z7_core_C` at 3600 min. *Checkpoint:* 98.3 % and 97.3. Trim 5.2 °C, surface 780.0 °C, core 775.7 °C.

(b) Press Reset, set Control architecture to + Core cascade and run again. *Checkpoint:* 99.0 % and 97.9. Trim 9.6 °C, surface 784.5 °C, core 780.1 °C.

(c) Explain why the surface cascade leaves the core about 4.3 °C short, and name the estimator error that would make the core cascade the worse of the two. *Checkpoint:* The offset grows with $m_c C_p / K_{sc}$ and with the heating rate. A conductance $\hat{K}_{sc}$ set too high.

Accept temperatures within 0.1 °C.

11.10 Application area · 3 min

Equation (11.10) makes the surface contamination of a parcel grow in proportion to $g(T_s) = [1 + \exp((T_s - 420)/60)]^{-1}$.

(a) Evaluate g at 780, 600, 420 and 300 °C. *Checkpoint:* 0.0025, 0.047, 0.50 and 0.88.

(b) Say where in the plant residual lithium picks up carbonate and hydroxide, which instrument watches for it, and why the app understates the pickup. *Checkpoint:* The cooling section and below. A dew-point or carbon dioxide analyzer. The model stops near 420 °C.

11.11 Application area · 4 min

A plant manager weighs line speeds with Table 11.5, taking the specific energy per kilogram of gross product.

(a) Find the heater energy per day at 100, 120 and 125 %, and for the supervisory layer at 8.14 t/d and 1.300 kW h/kg. *Checkpoint:* 9724, 10235, 10307 and 10 582 kW h a day.

(b) Find the energy per extra tonne of good product from 100 to 120 %, compare it with the average, and say what 125 % buys. *Checkpoint:* About 419 kW h/t against 1602.

11.12 Review the agent · 5 min

An AI assistant is asked how to pass the graded challenge of Section 11.5.4 and replies as follows. “At the design point the busiest heater runs at 72 %, so the kiln has 28 % of heater headroom. Heater duty scales with throughput, so the line can run at $100/72 = 139$ % before a heater saturates. Set the conveyor to 130 %: gross production rises to about 7.9 t/d at design density, well above the 7.4 t/d target, and the zone loops will hold zone 7 within ± 3 °C.” Find the flaw and say how you would check it.